Behavioral Modeling of Solute Tracking in Microfluidics

Y. Zeng
ECE Dept.
University of Utah
Salt Lake City, UT
yiz@eng.utah.edu

F. Azizi
ECE Dept.
University of Utah
Salt Lake City, UT
farouk.azizi@utah.edu

C. H. Mastrangelo
ECE Dept.
University of Utah
Salt Lake City
mastrang@eng.utah.edu

ABSTRACT

We present a general behavioral simulation method for the approximate solution of lumped, pressure-driven, static and time-dependent solute and solvent transport in large microfluidic chips. The method is based on a one-dimensional discretization of the convection-diffusion equation that tracks solvent and solute transport using four dual-branch nodal quantities. A comparison of static and transient behavior of microfluidic dilution networks and a PCM signal generator indicates that the simulation results are in good agreement with the model simulations.

1. INTRODUCTION

The design of microfluidic systems with hundreds of dynamic on-chip components [1,2] poses a challenge because today there are no CAD tools able to simulate time dependent transport of solvent and solutes through complex chips inclusive of dispersion and convection. Present approaches based on 3D CFD tools are only able to solve for transport through elementary components hence inadequate for system-level simulation. The use of analytical macromodel elements [3-5] has been shown to dramatically simplify solute-tracking calculations, but this method has only been demonstrated in a restricted set of linear electrokinetic [9] and static transport problems [3-8].

In this paper we present a general simulation method for the approximate solution of pressure-driven linear and nonlinear, static and time-dependent solute and solvent transport in large chips using a lumped approach. The method uses a finite-difference discretization of the one-dimensional convection-diffusion equation [10]. Solvent and solute transport is calculated using four lumped nodal quantities: solvent pressure, solvent volumetric flow rate, solute concentration and solute current as shown in the one-dimensional capillary element shown in Fig. 1. The dependence of the solvent and solute branch currents on the pressure and concentration values is discussed in the sections below.

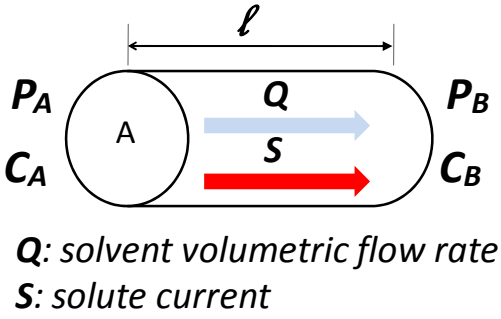

Fig. 1. Pressure-driven transport of solvent through a capillary results in solvent mass flow rate and solute currents.

2. LUMPED DUAL-BRANCH MODEL

In order to extract a lumped behavioral model we first consider the flow of a dilute solute and its solvent carrier through a simple capillary tube as depicted in Fig. 1. For practical purposes the dilute solute can be considered to be massless. The solvent flow, or volumetric flow rate is driven by a pressure difference between the two ends of the capillary. The solvent flow also convectively carries any solute within it. If the pressure difference is zero the solute itself can also diffuse or disperse as it moves forwad through the capillary tube. The solute diffusion is driven by concentration diffferences; therefore two driving forces: solvent pressure and solute concentration and two current quantities: solvent volumetric flow and solute current can be defined.

From first principles, the solute is represented by a space and time dependent concentration $c(x,y,z,t)$ flowing through the capillary with velocity $v(y,z)$. The solute concentration obeys a complex four dimensional convection diffusion PDE [11]. However if the capillary diameter is small relatively to its length ℓ, the problem is simplified when one considers the behavior of the average concentration $C(x,t)$ across its cross section under the influence of its average velocity V. The average concentration $C(x,t)$ approximately obeys the simplified, lumped one-dimensional convection-diffusion equation

$$D \cdot \frac{\partial^2 C}{\partial x^2} - V \cdot \frac{\partial C}{\partial x} = \frac{\partial C}{\partial t} \quad (1)$$

where D is the effective diffusion constant adjusted for Taylor-dispersion [12]. The solvent carrier is assumed to be incompressible hence its transport obeys the simplified Navier-Stokes equation which can also be averaged across the capillary cross section. This resuls in the one-dimensional solvent transport equation

$$-\beta_f \cdot Q - A \cdot \frac{\partial P}{\partial x} = \rho \frac{\partial Q}{\partial t} \quad (2)$$

where Q is the average volumetric mass flow rate, P is the driving pressure, ρ is the solvent density and A is the capillary area. The parameter β_f is related to the solvent hydraulic resistance which is a function of its viscosity μ and the capillary dimensions. For a rectangular capillary this is approximately [13]

$$\beta_f = \frac{12\mu w h^{-3}}{(\frac{w}{h}) - \sum_{m=0}^{\infty} (\frac{192}{\pi^5 (2m+1)^5}) \tanh[\frac{(2m+1)\pi w}{2h}]} \quad (3)$$

where w and h are the capillary width and height, respectively. Equations (1)-(2) uniquely determine the solute and solvent transport. Our model is based on a finite difference space discretization of these PDEs. This is done by slicing a capillary into smaller three-node differential elements element of length Δx shown in Fig. 2. The three-node element thus defines six internal and boundary nodal potential quantities $(P_{i-1/2}, C_{i-1/2})$, (P_i, C_i) and $(P_{i+1/2}, C_{i+1/2})$ and four branch flow quantities $Q_{i-1/2}$, $S_{i-1/2}$, $Q_{i+1/2}$, and $S_{i+1/2}$.

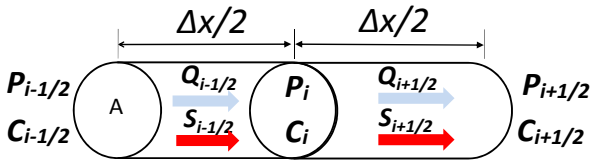

Fig. 2. Three-node discretization of a differential capillary element of length Δx with 6 nodal potential quantities and four branch flow quantities.

We used the following naive approximations

$$\frac{\partial^2 C_i}{\partial x^2} \approx \frac{4}{(\Delta x)^2} \cdot [C_{i+1/2} + C_{i-1/2} - 2C_i]$$
$$-V_i \frac{\partial C_i}{\partial x} \approx -\frac{V_i}{\Delta x} \cdot [C_i - C_{i-1/2}] \quad (4)$$

Other approximations can be used for improvements in convergence and stability [14]. Using Eq. (4) we arrive to the set of discrete equations

$$G_{st} \cdot (C_{i+1/2} - C_i) + G_{st} \cdot (C_{i-1/2} - C_i) + Q_{i-1/2} \cdot C_{i-1/2} - Q_{i+1/2} \cdot C_i = C_D \cdot \frac{dC_i}{dt} \quad (5)$$
$$(P_{i-1/2} - P_i) - R_f \cdot Q_{i-1/2} = L_f \frac{dQ_{i-1/2}}{dt}$$
$$(P_{i+1/2} - P_i) - R_f \cdot Q_{i+1/2} = L_f \frac{dQ_{i+1/2}}{dt}$$

where

$$G_{st} = \frac{4DA}{\Delta x}, R_f = G_{sv}^{-1} = \frac{\beta_f \cdot \Delta x}{2A}, C_D = A \cdot \Delta x, L_f = \frac{\rho \cdot \Delta x}{2A} \quad (6)$$

Furthermore, if the capillary walls are flexible, such as those in widely used PDMS chips, the element volume is dependent on the pressure thus resulting in the fourth equation

$$Q_W = \frac{dV_{ol}}{dt} = \frac{dV}{dP_i} \cdot \frac{dP_i}{dt} = C_W \cdot \frac{dP_i}{dt} \quad (7)$$

where C_W is the capillary wall compliance [15]. Equations (5)-(7) describe a lumped network shown in Fig. 3. The top

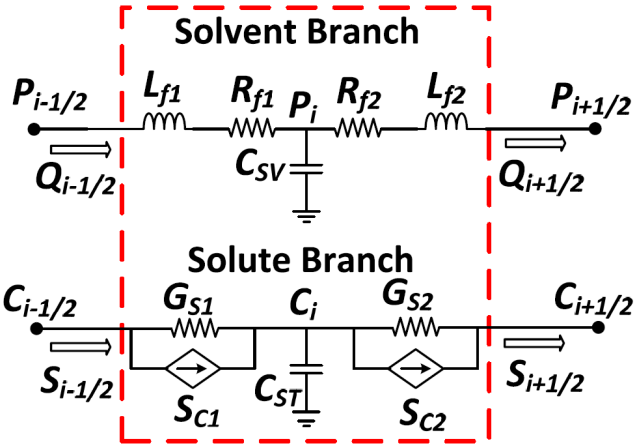

Fig. 3. Lumped two-branch network model for the capillary element.

branch models the transport of solvent while the bottom branch determines the transport of solute. The capacitive elements in each branch represent storage of solvent (for compressible wall structures) and solute, respectively. Each capillary in a chip is hence modeled as a series connection of N basic 4-terminal elements as shown in Fig. 4. The lumped model of Fig. 3 can be implemented in a hardware

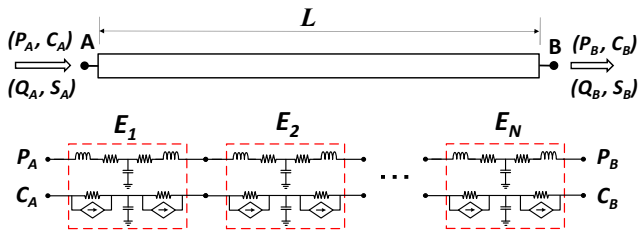

Fig. 4. Equivalent network for a capillary consisting of N elements.

language such as Verilog-AMS, and the entire chip is specified by a component connectivity netlist.

3. VERILOG-AMS IMPLEMENTATION

The two-branch, four port model of Fig. 3 is controlled by two potential-like quantities (solvent pressure and solute concentration) and two corresponding flow quantities (solvent volumetric flow and solute current) at its terminals. The mixed nature of the state variables is suitable for coding the element behavior in Verilog-AMS. In Verilog-AMS, the state variable units and their corresponding relations are first defined. The nature of Solvent and Solute variables is shown in the simplified Listing 1 below for the file *disciplines.vams*.

Listing 1. Flow Variable Natures

```
// Solvent  "potential" and "flow" quantities are Psv and Qsv
// Solute   "potential" and "flow" quantities are Cst and  Sst

// Solvent quantities
nature SolventCurrent
    units = "-nL/s" ;
    access = Qsv ;
    idt_nature = SolventVolume ;
endnature
nature SolventPressure
    units = "Pa" ;
    access = Psv ;
endnature

// Solute quantities
nature SoluteCurrent
    units = "Molec/s" ;
    access = Sst ;
endnature
nature SoluteConcentration
    units = "Molec/nL" ;
    access = Cst ;
endnature

// define discipline bindings (both are conservative)
discipline Solvent
    domain continuous;
    potential SolventPressure ;
    flow SolventCurrent ;
enddiscipline
discipline Solute
    domain continuous;
    potential SoluteConcentration ;
    flow SoluteCurrent ;
enddiscipline
```

The central element in the simulation scheme is the one-element capillary of Fig. 3 requiring the definition of fluid-solute-tracking resistors, capacitors and inductors. This results in the simplified code of Listing 2 below. In Listing 2, each element module has two Solvent nodes (a,b) and two Solute nodes (c,d). The module *FlowResistor* also includes the convective transport term Qsv(a,b)*Co. The convective term uses the solute concentration of one of the nodes such that the solute flows *into* the element. This scheme suppresses oscillations and improves numerical convergence.

Listing 2. Simplified Flow Resistor, Capacitor and Inductor Models.

```
`include "disciplines.vams"

module FlowResistor(a,b,c,d);  // includes all resistive/conv. transport
inout a, b; c, d;
Solvent a, b;
Solute c, d;
real CL, CR; Co;
analog begin
CL = Cst(c);
CR = Cst(d);
 if ( Psv(a,b) >= 0.0 ) begin  // select the concentration moving forward
        Co = CL;
 end
 if ( Psv(a,b) < 0.0) begin
        Co = CR;
end
Qsv(a,b) <+ Gsv * Psv(a,b);   // solvent pressure-mass-flow relation
Sst(c,d) <+ Gst*Cst(c,d) + Qsv(a,b)*(Co);  //solute  diffusion + convection
end
endmodule

module FlowCapacitor(a,b,c,d);  // includes both solvent and solute
inout a, b, c, d
Solvent a, b;
Solute c, d;
analog begin
Psv(a,b) <+ 1.0/cc_compliance*idt(Qsv(a,b)); // define solvent capacitor
Cst(c,d) <+  volume*idt(Sst(c,d));  // define solute capacitor
end
endmodule

module FlowInductor(a,b,c,d);  // includes both solvent and solute
inout a, b, c, d
Solvent a, b;
Solute c, d;
analog begin
area = w*h;
Lf = density*l/area;
Qsv(a,b) <+ 1//Lf*idt(Psv(a,b)); // define solvent  inductor
Cst(c,d) <+ 0.0;                 // define solute short circuit
end
endmodule
```

The module *FlowCapacitor* accounts for the solute storage in the element volume and the capillary wall

compressibility through the compliance parameter. Finally the module *FlowInductor* accounts for the inertial forces of the solvent mass stored in the capillary element. The simplified code of Listing 2 does not account for static transport changes originated by capillary and fluid elasticity, but the code can be easily adapted to include this effect. For thick-walled capillaries [16, 17] such as those present in PDMS devices, the compliance parameter C_M is approximately

$$C_M \approx \frac{9}{4 \cdot E_W} + \frac{1}{E_f} \tag{8}$$

where E_w and E_f are the wall material Young's modulus and fluid bulk modulus, respectively.

In order to simulate solute-tracking transport in a complex microfluidic chip a nodal netlist is first generated. The entire chip description can then be simulated using a Verilog-AMS simulator such as Synopsys' HSPICE or Dolphin's SMASH. In the section below we discuss several specific examples. All transient simulations were carried out using a robust backward Euler scheme.

4. SIMULATION EXAMPLES AND COMPARISON WITH EXPERIMENTS

In order to evaluate the proposed model we next compare the simulation results to experimental and theoretical values for several microfluidic chips.

4.1 Binary Dilution Network

The first chip consists of a binary dilution network described in [18]. Such 19-capillary network, as shown in Fig. 5 below provides multiple static outputs of equal volumetric flows of a solute with binary-weighted concentrations.

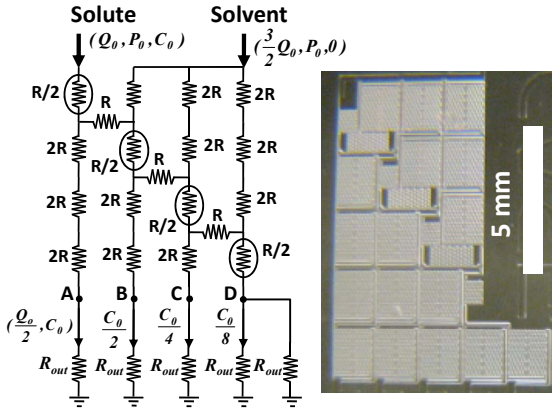

Fig. 5. Photograph and schematic of a PDMS binary dilution network [18].

Mixing and dilution takes place in the encircled flow capillaries. The capillary dimensions for the resistor R is $50\times16\times1500$ μm^3. Each capillary in the chip is modeled as a series connection of 5 differential elements.

Table 1. Comparison of normalized bit concentrations

	A	B	C	D
Theory	1.0	0.5	0.25	0.125
Simulation	1.0	0.49	0.249	0.1248
Experiment	1.0	0.49	0.24	0.105

The solute was a solution of fluorescein disodium dye in H_2O (0.1 mg/ml) and the drive pressure was about 10 PSI. Table 1 shows the comparison of theoretical, simulated and experimental relative concentrations are in good agreement.

4.2 Switching Gradient Generator

The simulator was next used to analyze a 72-capillary, PDMS gradient generator [19,20] shown in Fig. 6 with equivalent 53-node, 7-output lumped network. The chip is

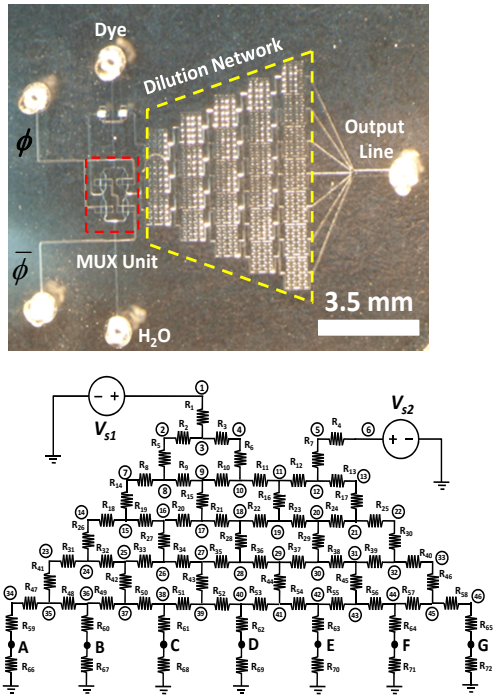

Fig. 6. Photograph and network schematic of a PDMS chemical gradient generator.

driven by alternating flows of dye and water using a four-valve multiplexer (MUX) unit causing the direction of the gradient to switch (at constant solvent flows). The capillary dimensions were 25×16 μm^2. We fabricated and tested this PDMS chip using the methods described in [18].

Fig. 7 shows the chip in operation using fluorescein disodium (0.1 mg/ml) as the analyte. Static and time

dependent fluorescence intensity at different locations in the chip were recorded with an Olympus MVX10

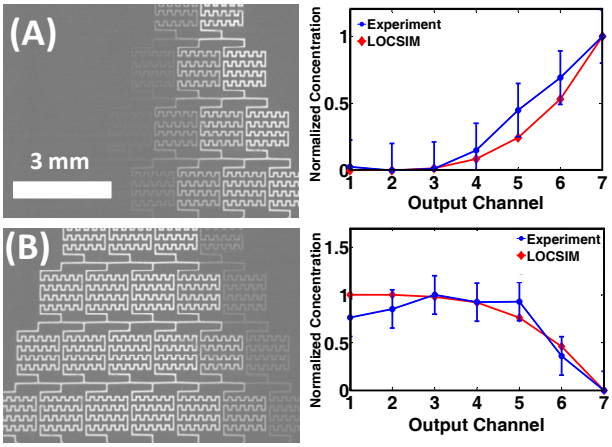

Fig. 7. Comparison of experimntal and simulated normalized, static dye concentration at the output channels of the gradient generator

fluorescence microscope and Hamamatsu EM-CCD intensified camera. Fig. 8 shows simulated and experimental output concentrations under periodic excitation. The simulation run, tracking the dynamic behavior of 5200 nodal quantities, was completed in three minutes in a PC laptop.

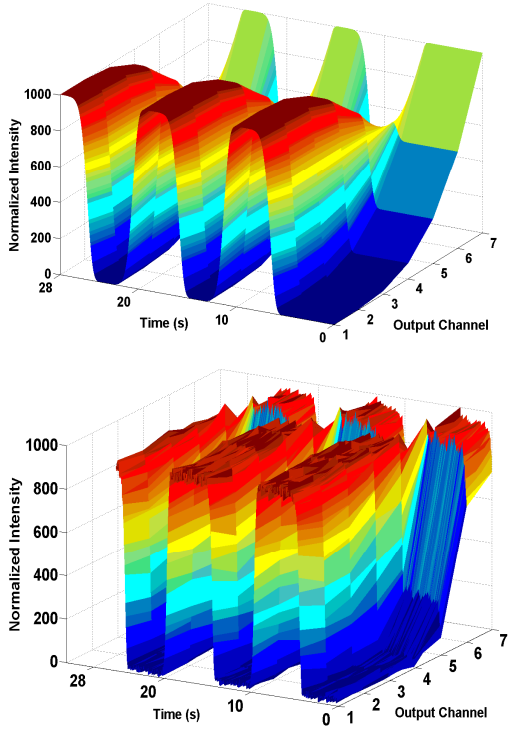

Fig. 8. Comparison of simulation (top) of dynamic output gradients for the chip of Fig. 6 and experimental results (bot). The chip solute inputs were switched at 0.1 Hz.

4.3 Pulse Coded Modulators

In the last example we simulated the output of a microfluidic pulse coded modulator (PCM) [21]. In a PCM chip, solute plugs of fixed concentration are introduced at high rate into a long capillary which disperses and mixes the plugs. The mixing effect essentially produces an average output concentration proportional to the plug density. Fig. 9 shows the schematic of a simple microfluidic PCM consisting of two valves represented as switches and a long capillary at the exit. The valves are driven by digital clock ϕ so that at any given time either pure solvent (lower valve open, upper closed) or solvent plus solute (upper valve open, lower valve closed) flows but not both, thus producing a series of solute plugs in the flow. The number of plugs is determined by a digital code over a repeating cycle. The concentration at the output of the PCM approaches a steady value that is proportional to the PCM code.

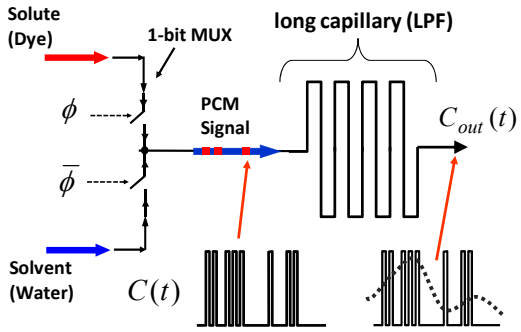

Fig. 9. One-bit microfluidic PCM. The long capillary averages the plugs producing a smooth solute concentration signal.

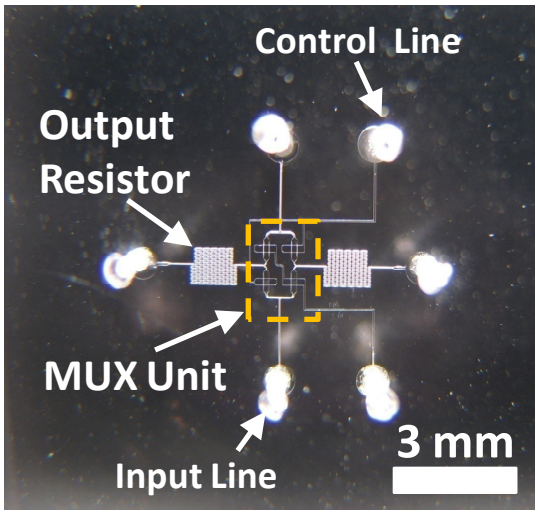

Fig. 10. One-bit PCM chip

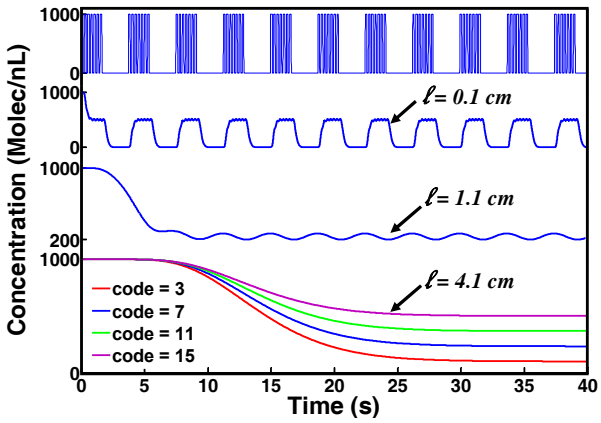

Fig. 11. Simulated solute concentration waveforms for a 1-bit PCM chip for different codes and at different lengths from the multiplexer exit. The capillary width is 50 µm. The top three trace shows the waveforms for PCM code 7/15.

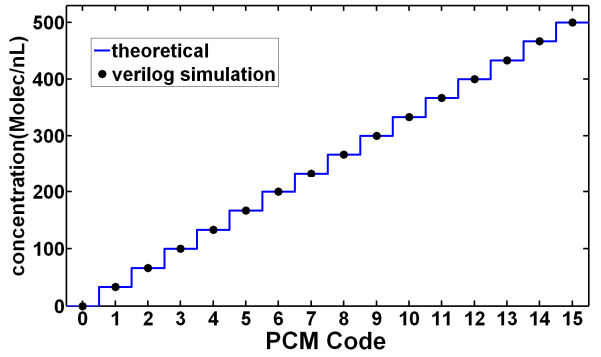

Fig. 12. Comparison of theoretical (blue) and verilog-AMS simulated PCM output solute concentration versus input code.

Fig. 10 shows a photograph of an example dual one-bit PCM PDMS chip with two output capillaries fabricated by our group. Other more complex PCM chips are discussed in [21]. Fig. 11 shows example simulated waveforms for a one-bit PCM chip with a capillary length of 51 mm. Fig. 12 shows the simulated output level versus code compared to the theoretical response. The two curves match well with good agreement.

5. SUMMARY

This paper presents a general behavioral simulation method for the approximate solution of lumped pressure-driven linear and nonlinear, static and time-dependent solute and solvent transport in large microfluidic chips. A comparison of simulated and experimental static and transient behavior of microfluidic dilution networks and a PCM signal generator are in good agreement.

6. REFERENCES

[1] J. P. Urbanski, W. Thies, C. Thodes, and S. Amarshinge and T. Thorsen, *Lab Chip*, 2005, 6, 96-104.

[2] A. M. Amin, M. Thottethodi, T. N. Vijaykumar, S. T. Wereley, S. C. Jacobson, *µTAS 2007,* 967-969.

[3] A. Chatterjee and N. R. Aluru, *JMEMS*, 2005, 14, 81-95.

[4] Y. Wang, Q. Lin and T. Mukherjee, *Lab Chip*, 2004, 4, 453-463.

[5] Y. Wang, Q. Lin and T. Mukherjee, *Lab Chip*, 2004, 5, 877-887.

[6] T. Mukherjee, *IEEE ICCAD-2005*, 463-470.

[7] Y. Wang, Q. Lin and T. Mukherjee, *IEEE BMAS* 2004, 8-13.

[8] Y. Wang, T. Mukherjee and Q. Lin, J. *Micromech. Microeng.*, 16, 2006, 2128-2137.

[9] D. Vasilyev, M. Rewienski and J. White, *IEEE TCAD*, 24, 2006, 285-290.

[10] A. Y. Layton, *J. Biol. Sys*., 13, 2005, 151-172.

[11] N. Nguyen and X. Huang, *Lab Chip*, 2005, **5**, 1320.

[12] D. A. Beard, *J. of Appl. Physics*, 2001, **89**, No. 8, 4667-4669.

[13] W.E.Marf et.al. *Sensors and Actuators B.* 2001, **72**, 266-272.

[14] Y. Shapira, *Solving PDEs in C++,* SIAM, Philadelphia, 2006.

[15] M. R. Bageley and M. Utz, *µTAS 2008*, 1351-1353.

[16] L. A. Taylor and J. H. Gerrard, Med. & Biol. Eng. & Comput., 1977, 15, 11-17.

[17] K. S. Matthys, *Assessment of Vascular Haemodynamics,* PhD Thesis, University of Ghent, 2003.

[18] L. Chen, F. Azizi, C. H. Mastrangelo, *Lab Chip*, 2007, 7, 850-855.

[19] S. K. W. Dertinger, D. T. Chiu. N. L. Jeon and G. M. Whitesides, *Anal. Chem.,* **2001**, 73(6):1240-1246

[20] F. Lin, W. Saadi, S. W. Rhee, S. Wang, S. Mittal and N. L. Jeon, *Lab Chip*, 2004**,** 4, 164-167.

[21] F. Azizi and C. H. Mastrangelo, *Lab Chip*, 2008, 6, 907-912.